ELSEVIER

Contents lists available at ScienceDirect

New BIOTECHNOLOGY

journal homepage: www.elsevier.com/locate/nbt



Microbial synthesis of polyhydroxyalkanoate blends with engineered *Pseudomonas putida*

Minglong Li^a, Khalid Doudin^b, David B. Robins^a, Georgios Tetradis-Mairis^c, Tuck Seng Wong ^{a,d,e,f,*}, Kang Lan Tee ^{a,d,*}

- a School of Chemical, Materials & Biological Engineering, University of Sheffield, Sir Robert Hadfield Building, Mappin Street, Sheffield S1 3JD, United Kingdom
- b School of Mathematical and Physical Sciences, University of Sheffield, Dainton Building, Brook Hill, Sheffield, S3 7HF, United Kingdom
- ^c Nomad Foods Europe Limited, 43 Church Street West, Woking GU21 6HT, United Kingdom
- ^d Evolutor Ltd, The Innovation Centre, 217 Portobello, Sheffield S1 4DP, United Kingdom
- ^e National Center for Genetic Engineering & Biotechnology (BIOTEC), National Science & Technology Development Agency (NSTDA), 113 Thailand Science Park,
- Phahonyothin Road, Khlong Nueng, Khlong Luang, Pathum Thani 12120, Thailand ^f School of Pharmacy, Bandung Institute of Technology, Bandung, West Java, Indonesia

ARTICLE INFO

Keywords: Polyhydroxyalkanoate Polymer blends Pseudomonas putida Promoters Synthetic biology

ABSTRACT

Polyhydroxyalkanoates (PHAs) are biopolymers naturally produced by various microorganisms and offer a sustainable alternative to fossil fuel-derived plastics. They can be synthesized from diverse feedstock, including waste biomass such as lignocellulose, municipal waste, sludge, and industrial by-products. To tailor their properties for specific applications, PHAs are typically blended post synthesis. An alternative approach is the direct synthesis of PHA blends in a single fermentation, which can reduce the need for multiple separate fermentations and extractions. In this study, we engineered Pseudomonas putida to synthesize PHA blends composed of poly-3-hydroxybutyrate [P3(HB)] and medium-chain-length PHA (mcl-PHA). Through using different promoters, blends with 3HB monomer content ranging from 17.9 mol% to 99.6 mol% were produced. Optimizing cultivation conditions yielded a maximum PHA production of 1.48 \pm 0.15 g/L, with a PHA content of 52.2 ± 4.3 wt% of cell dry weight. A combination of gel permeation chromatography, nuclear magnetic resonance and diffusion ordered spectroscopy were employed to determine the molecular weight and confirm the identity of the PHA blend, revealing in all cases, a higher molecular weight P(3HB) than mcl-PHA. The blends produced had thermal properties comparable to PHA blends produced by post synthesis melt compounding. This work demonstrates the microbial synthesis of PHA blends in P. putida and is the first instance of blend composition control via promoter selection, paving the way for the one-step biomanufacturing of customizable PHA blends.

1. Introduction

Polyhydroxyalkanoate (PHA) is a family of bio-based and biodegradable polyesters naturally produced by bacteria and archaea. These diverse species have been summarised in numerous reviews and key examples include *Cupriavidus necator*, *Pseudomonas putida*, *Bacillus subtilis* and *Haloferax mediterranei* [1–4]. PHAs are broadly categorized into short-chain-length PHA (scl-PHA) or medium-chain-length PHA (mcl-PHA), based on the 3–5 carbons or 6–14 carbons in the 3-hydroxyalkanoic monomers respectively. The potential of PHA as a biomaterial of the future is widely researched, with many excellent reviews on

their biosynthesis, characteristics and applications, as well as engineering strategies to control their properties and improve manufacturing [5–8].

In Nature, the type of PHA a bacterium produces is defined by its metabolic pathways. In scl-PHA synthesis, three key enzymes (PhaA, PhaB and PhaC) are involved, as seen in the well-studied PHB producing bacterium *Cupriavidus necator* H16 (Figure S1). PhaA catalyses the condensation of two acetyl-CoA molecules into acetoacetyl-CoA, which is then converted to (*R*)-3-hydroxybutyryl-CoA by PhaB. This intermediate is subsequently polymerised by PhaC into P(3HB). In contrast, mcl-PHA is synthesized via precursors generated by two metabolic

E-mail addresses: t.wong@sheffield.ac.uk (T.S. Wong), k.tee@sheffield.ac.uk (K.L. Tee).

^{*} Corresponding authors at: School of Chemical, Materials & Biological Engineering, University of Sheffield, Sir Robert Hadfield Building, Mappin Street, Sheffield S1 3JD, United Kingdom.

Table 1
Plasmids used in this study.

Plasmid	Description	Source or reference	
pBBR1-MCS2	Broad-host-range vector, Km ^R	[29]	
Pj5-RFP	oriV(pBBR1); P _{i5} -rfp. Cam ^R	[28]	
Pg25-RFP	oriV(pBBR1); P _{g25} -rfp. Cam ^R	[28]	
PrrsC-RFP	oriV(pBBR1); P _{rrsC} -rfp. Cam ^R	[28]	
PphaC1-RFP	oriV(pBBR1); P _{phaC1} -rfp. Cam ^R	[28]	
Pj5k-RFP	Pj5-RFP derived, P _{i5} -rfp. Km ^R	This study	
Pg25k-RFP	Pg25-RFP derived, P _{g25} -rfp. Km ^R	This study	
PrrsCk-RFP	PrrsC-RFP derived, P _{rrsC} -rfp. Km ^R	This study	
PphaC1k-RFP	PphaC1-RFP derived, PphaC1-rfp. Km ^R	This study	
pBBR1c- phaCAB	oriV(pBBR1); C. necator phaCAB. Cam ^R	Lab collection	
PphaC1k- phaCAB	PphaC1-RFP derived, <i>C. necator phaCAB</i> . Km ^R	This study	
pPS85	oriV(pBBR1); araC-ParaB-gfp(Mut3). Gm ^R	[30]	
pPS87	oriV(pBBR1); rhaS-rhaR-PrhaB-gfp (Mut3). Gm ^R	[30]	
ParaB-phaCAB	pPS85 derived, C. necator phaCAB. GmR	This study	
PrhaB-phaCAB	pPS87 derived, C. necator phaCAB. GmR	This study	

pathways, namely β -oxidation and fatty acid synthesis (Figure S1). Across all pathways, the substrate specificity of PHA synthase (PhaC) determines the monomer composition of the synthesized PHA. Some PhaCs only incorporate scl-PHA monomers, like the PhaC from *C. necator* H16 which produces P(3HB) homopolymer. Others will polymerize only mcl-PHA monomers, exemplified by the PhaC from *Pseudomonas putida*. While rare, PhaCs that accept substrates for both scl- and mcl-PHA have been identified [9,10], though their substrate range is limited to monomers with 4–6 carbons, like the PhaC from *Aeromonas caviae* [10].

PHA monomer composition influences its physical and mechanical properties. For instance, poly(3-hydroxybutyrate) [P(3HB)] homopolymers are stiff and brittle thermoplastics. In contrast, poly(3hydroxyoctanoate) [P(3HO)] homopolymers are sticky and ductile making them suitable as elastomer materials [11]. Two common methods for modulating the properties of naturally produced PHA are copolymerisation and polymer blending. Copolymers can be produced through feedstock design and feeding strategy or production strain engineering [12,13], with a few examples of copolymers with scl-PHA and mcl-PHA synthesized in engineered Escherichia coli [14,15]. Compared to copolymerisation, PHA blending is a more widely used approach. P (3HB) and P(3HO) blends showed higher tensile strength and Young's modulus compared to P(3HO) alone [16], and better thermal stability PHB compared to alone [17]. P(3HB) and (3-hydroxybutyrate-co-3-hydroxyhexanoate) blends have been used to produce scaffolds for use as a matrix for cartilage tissue engineering [18-20] and blends of PHA with other polymers have been spun into fibres and processed into trays and films with high gas and liquid barrier capabilities [21]. Typically, PHA blends are created by combining individual purified PHAs, as it is rare to find bacteria that naturally produce a PHA blend. A unique example is Pseudomonas umsongensis GO16, which synthesizes a blend of P(3HB) and P(3HO) [22]. Other approaches to fermentative production of PHA blends include co-cultivation of two different bacteria [23] or a bacteria consortium in activated sludge [24].

In this study, *Pseudomonas putida* was engineered to produce a blend of scl-PHA and mcl-PHA. This was achieved by introducing the *phaCAB* operon from *Cupriavidus necator* H16 to *P. putida*. One significant advantage of this approach is the ability to control the composition of the PHA blend by fine-tuning gene expression in the scl-PHA and mcl-PHA pathways. *P. putida* is a natural producer of mcl-PHA and identified as the production host due to its versatile metabolism, rapid growth, ability to withstand harsh conditions, and its non-pathogenic nature, making it an ideal candidate for industrial-scale bioproduction [25].

2. Material and methods

2.1. Bacterial cultivation and transformation

Escherichia coli DH5α was used for molecular cloning, plasmid propagation, and maintenance. Pseudomonas putida mt-2 (DSM 6125; DSMZ, Braunschweig, Germany) was used for PHA production. E. coli was cultivated in Luria–Bertani (LB) medium (10 g/L tryptone, 5 g/L yeast extract, 10 g/L NaCl) at 37°C. P. putida was cultivated at 30°C in either LB medium or mineral salt medium (MSM) supplemented with 1 %(w/v) – 6 %(w/v) glucose as the sole carbon source. Glucose concentration of 1 %(w/v) was used unless stated otherwise. MSM was prepared as previously described [26] with a reduced concentration of nitrogen (0.5 g/L NH4Cl). The TYE agar (10 g/L tryptone, 5 g/L yeast extract, 8 g/L NaCl, 15 g/L agar) was used for both E. coli and P. putida. Kanamycin (50 μg/mL) and gentamicin (20 μg/mL) were supplemented when required. Optical density (OD600) was measured at 600 nm (WPA CO 8000 Cell Density Meter, Biochrom Ltd, England).

The standard calcium chloride method was used to transform plasmids into DH5 α while a modified electroporation method was used for *P. putida* [27]. Briefly, a fresh colony was used to inoculate 5 mL of LB. Cells were cultivated overnight at 30°C with shaking at 250 rpm for this pre-culture. Electrocompetent cells were prepared by transferring 400 μ L of pre-culture to 20 mL of LB. Cells were cultivated to an OD₆₀₀~0.6, chilled on ice for 10 min and harvested by centrifugation (5000 g, 10 min and 4°C). The cell pellet was washed twice with ice-cold 10 %(v/v) glycerol and resuspended in 1 mL of 10 %(v/v) glycerol. One microliter of plasmid DNA was added to 100 μ L of competent cells, transferred to a pre-chilled 2-mm electroporation cuvette and electroporated at 2.3 kV (Eppendorf Eporator, Eppendorf, Germany). The cells were then resuspended by adding 900 μ L of LB, incubated at 30°C with shaking for 2 h, before plating on TYE agar plate with the appropriate antibiotic. A schematic of the workflow is shown in Figure S2.

2.2. Molecular cloning of plasmids for promoter test and PHA production

All plasmids used in this study are listed in Table 1. Plasmids with constitutive promoters were constructed using previously reported plasmids [28]. In brief, the chloramphenicol acetyltransferase selection marker on plasmids PphaC1-RFP, PrrsC-RFP, Pj5-RFP and Pg25-RFP was replaced with the aminoglycoside phosphotransferase gene from pBBR1MCS-2 for kanamycin resistance [29]. These four plasmids were amplified using primers PB-F and PB-R. The aminoglycoside phosphotransferase gene was amplified using primers Km-F and Km-R. Amplified products were purified with the Gel and PCR Clean-Up Kit (Macherey-Nagel, Germany) and fragments were assembled by using NEBuilder HiFi DNA Assembly Master Mix (New England Biolabs, UK) according to the manufacturer's protocols to create PphaC1k-RFP, PrrsCk-RFP, Pj5k-RFP and Pg25k-RFP. Plasmids pPS85 (with ParaB promoter) and pPS87 (with PrhaB promoter) for inducible protein expression in P. putida were obtained from the pSEVA-sib collection [30]. All oligonucleotide primers used for PCR amplification are listed in Table S1 (Eurofins, Germany).

For P(3HB) production in *P. putida*, the *Cupriavidus necator* H16 *phaCAB* operon was amplified from plasmid pBBR1c-phaCAB with primers phaCAB-F and phaCAB-R, and used to create plasmids ParaB-phaCAB, PrhaB-phaCAB and PphaC1k-phaCAB by NEBuilder HiFi DNA Assembly before transformation into *P. putida*.

2.3. Promoter strength assay

A single colony of transformed *P. putida* was transferred into 5 mL of LB medium and incubated overnight at 30° C, 250 rpm. This pre-culture was used to inoculate 5 mL of fresh MSM medium to an initial OD₆₀₀ of 0.2. The cells were cultivated at 30° C, 250 rpm. For constructs with inducible promoters, 0.4 %(w/v) arabinose or 10 mM rhamnose was

added to induce fluorescent protein production when $OD_{600}\sim0.6$. At fixed intervals (4 h, 8 h, 12 h, 16 h, 20 h, 24 h, 48 h, 72 h), $100~\mu L$ of cells was transferred into a 96-well clear bottom plate for fluorescence measurement of RFP (Ex 584 nm, Em 607 nm) or GFP (Ex 485 nm, Em 528 nm) using the SpectraMax M2e microplate reader (Molecular Devices, UK).

2.4. PHA production for composition analysis

A single colony of wild type *P. putida* or transformant was transferred into 20 mL of LB medium and incubated overnight at 30°C, 250 rpm. This pre-culture was used to inoculate 400 mL of fresh MSM medium to an initial OD_{600} of 0.2. The cells were cultivated at 30°C, 250 rpm. At $OD_{600} \sim 0.6$, the *phaCAB* operon was induced using either 0.4 %(w/v) of arabinose or 10 mM of rhamnose. For composition analysis, 50 mL of cells were harvested at fixed intervals (12 h, 16 h, 20 h, 24 h, 48 h) by centrifugation (8000 rpm, 10 min). All cell pellets were washed twice with 1 × phosphate-buffered saline solution (137 mM NaCl, 2.7 mM KCl, 8 mM Na₂HPO₄, and 2 mM KH₂PO₄), frozen at -80° C and lyophilised. The lyophilised cells were weighted to obtain the cell dry weight (CDW). Intracellular PHA content of lyophilised cells was analyzed using gas chromatography.

2.5. PHA production and Soxhlet extraction

Cells were cultivated as in PHA production for composition analysis, except all cells were harvested after 24 h of cultivation and lyophilised. The lyophilised cells were transferred to an extraction thimble for Soxhlet extraction. The sample was first refluxed in 90 mL of methanol for 2 h followed by 100 mL of dichloromethane for at least 12 h. The PHA in dichloromethane was concentrated and precipitated in 50–100 mL of cold methanol. If necessary, the PHA was re-dissolved in dichloromethane and precipitated again to further improve its purity.

2.6. Gas chromatography (GC) analysis of PHA

Ten milligrams of lyophilized cells or PHA were subjected to methanolysis for 3.5 h at 100°C in dichloromethane, methanol and sulphuric acid in the volume ratio of 2.0:1.7:0.3 respectively. Benzoic acid (1 mg/ mL) was added as an internal standard. The 2 mL reaction was then cooled in ice and 1 mL of distilled water was added. This mixture was vortexed for 5 min and left to stand to allow phase separation. The organic phase was analyzed by gas chromatography with the Shimadzu GC2010 pro (Kyoto, Japan) equipped with a SH-Rtx-5MS column (30 m \times 0.25 mm \times 0.5 μ m; Shimadzu) and a flame ionization detector. One microliter of each sample was injected into the GC with a split ratio of 100:1 (vent:column). Hydrogen was used as the carrier gas at a flow rate of 40 mL/min. The oven was held at 80°C for 5 min, heated from 80 to 180°C at 8 °C/min and held at 180°C for 12 min. Standards of 3-hydroxy methyl esters for monomers with 4-12 carbons (Cayman Chemical Company, USA) were used to generate calibration curves for quantification.

2.7. Gel permeation chromatography

PHA extracted by Soxhlet was used for molecular weight determination through gel permeation chromatography (GPC). One hundred microliters of sample (1–3 mg/mL) were analysed on an Agilent 1260 Infinity LC system (Agilent, USA), equipped with a refractive index and viscosity detector. Polymers were separated using two PLgel MIXED-C (7.5 \times 300 mm, 5 μm ; Agilent) columns with a PLgel guard column (7.5 \times 50 mm, 5um; Agilent), all connected in series. Chloroform was used as the mobile phase at a flow rate of 1 mL/min, with the columns maintained at 40°C. Low-polydispersity polystyrene standards with peak molecular weights ranging from 0.162×10^3 to 1.014×10^6 g/mol (InfinityLab EasiVial Standards, Agilent) were used as standards. All

molecular weight standards and experimental samples contained toluene as an internal standard to normalize retention times. Calibration of the system and analysis of the experimental samples were performed using the Agilent GPC data analysis software package. The number-average molecular weight (Mn), weight-average molecular weight (Mw), and polydispersity (PD) were measured for each sample.

2.8. Thermogravimetric analysis of PHA

Thermal degradation was evaluated using a Perkin Elmer PYRIS 1 TAG system. Approximately 8 mg of PHA sample was heated from 30°C to 400°C at a rate of 10°C/min under a nitrogen stream with a flow rate 20 mL/min. The thermogravimetric and derivative thermogravimetric curve was used to determine the degradation onset temperature (T_{onset}) and degradation temperature (T_{d}).

2.9. Differential scanning calorimetry of PHA

The thermal properties of PHA were analyzed by differential scanning calorimetry (DSC), using the Perkin Elmer DSC4000 system under a nitrogen stream with a flow rate 20 mL/min. Each PHA sample (5–7 mg) was placed in an aluminium pan and held at -80°C for 1 min. In the first heating cycle, the sample was heated from -80°C to 200°C at 10°C/min and held at 200°C for 1 min. The sample was then cooled from 200°C to -80°C at 5°C/min and held at -80°C for 5 min. For the second heating, the sample was heated again from -80°C to 200°C at 10°C/min . The crystallization (T_{c}) temperature and the enthalpy of crystallization (ΔH_{c}) was obtained from the DSC curve of the cooling step. The melting temperature (T_{m}) and enthalpy of melting (ΔH_{m}) was obtained from the DSC curve of the second heating.

2.10. Nuclear magnetic resonance of PHA

 ^{1}H spectra were recorded on Bruker Avance AVIII 400 MHz NMR spectrometers equipped with a 5-mm solution state BBO probe with Z-gradient, the temperature was regulated at 25°C and no spinning was applied to the NMR tube. Standard ^{1}H experiments were measured at 400.13 MHz using a 30° pulse for excitation, 64 k acquisition points over a spectral width of 20 ppm with 16 transients and a relaxation delay of 1 s. Chemical shifts are given in ppm with respect to tetramethylsilane using the NMR solvent used as internal standards.

For diffusion ordered spectroscopy (DOSY), 1H DOSY NMR spectra were recorded on Bruker Avance AVIII 400 MHz NMR spectrometers equipped with a 5-mm solution state BBO probe with Z-gradient at temperature 25C. Using the standard single-stimulated echo pulse sequence stebpgp1s, the pulsed-field gradients were incremented in 16 steps, from 5 % to 95 % of the maximum gradient strength (3.4 G/cmA) in a linear ramp and 32 scans at each step. The diffusion time Δ (d20) and the gradient length δ (p30) were optimized for each sample. The DOSY spectra were multiplied with an exponential window function before Fourier transformation (xf2) and subsequently phase and baseline corrected.

Diffusion coefficient (D) for each sample was obtained using Diffusion in Dynamics Center software and fitting each curve using Eq. (1) below:

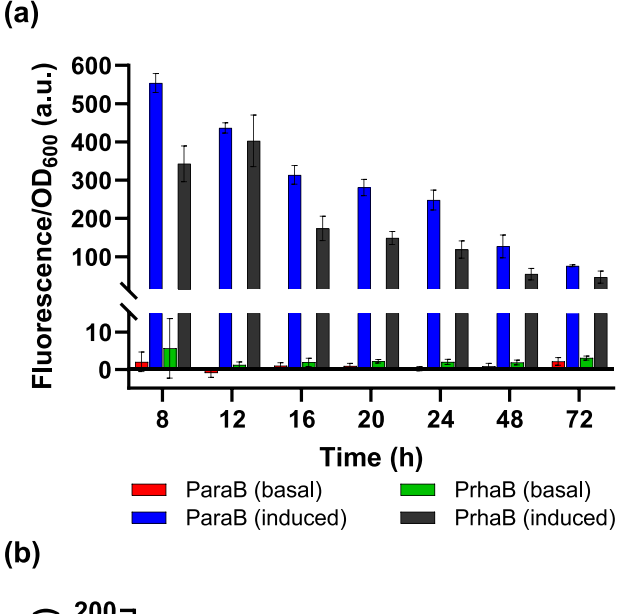
$$I = I_0 e^{\left[-D\gamma^2 g^2 \delta^2 (\Delta - \delta/3)\right]} \tag{1}$$

where, I is signal intensity, I_0 is the reference intensity, D is diffusion coefficient, γ is the gyromagnetic ratio of the observed nucleus, g is the gradient strength, the little delta δ is the length of the gradient and the big delta Δ is the diffusion time.

2.11. Potato peel hydrolysate preparation

Potato peel waste from Nomad Foods Limited sites in Lowestoft (UK)

New BIOTECHNOLOGY 88 (2025) 161-170



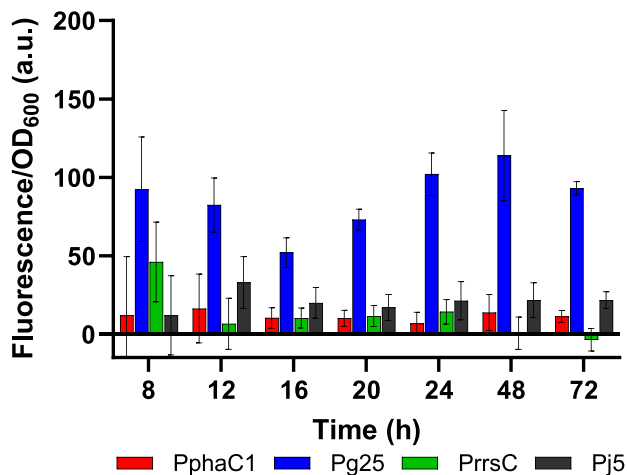


Fig. 1. Activity of six different promoters in *P. putida*. For promoter activity measurement, cells (100 μ L) were transferred to a microplate for fluorescence detection. (a) Cells carrying plasmids were induced with 0.4 %(w/v) arabinose for the ParaB promoter and with 10 mM rhamnose for the PrhaB promoter. Basal activities were measured for non-induced cells. Cells were sampled at intervals between 8 h to 72 h after induction (b) Cells carrying plasmids with the constitutive promoters were sampled between 8 h and 72 h after inoculation. All cultivation was conducted at 30°C. Background fluorescence from *P. putida* without plasmid was subtracted from all data and fluorescence readings were normalized to the optical density of the culture.

was dried and milled into particles of <1 mm and hydrolysed using a two-step enzymatic method. Briefly, 20 g of potato peel powder was mixed with 200 mL of deionized water, and the pH was adjusted to 6.0 using NaOH. Subsequently, 2 mL of BAN 480 L (Sigma-Aldrich), an α -amylase from <code>Bacillus</code> amyloliquefaciens, was added to the mixture and incubated at 80 °C for 30 minutes with intermittent mixing. After incubation, the pH was adjusted to 4.0 using sulphuric acid, followed by the addition of 2 mL of AMG 300 L (Sigma-Aldrich), a glucoamylase from <code>Aspergillus</code> niger. The mixture was further incubated at 60 °C for 30 minutes. The liquid hydrolysate was separated by filtration and centrifugation. The pH of the resulting supernatant was adjusted to 7.0 and autoclaved. The final potato peel hydrolysate was diluted with either sterile deionized water or MSM medium at a 1:1 (v/v) ratio and used as media for cell cultivation and PHA production.

Glucose and xylose concentrations in the hydrolysate were determined by high-performance liquid chromatography (HPLC) using the

Prominence-i LC-2030C Plus (Shimadzu UK Ltd., Milton Keynes, UK) equipped with a Rezex RCM-Monosaccharide column (300 \times 7.8 mm; Phenomenex, Macclesfield, UK) and a refractive index detector. Ten microliters of sample were injected using an autosampler and isocratic separation was achieved at 60 $^{\circ}\text{C}$ using water flowing at 0.6 mL/min as the mobile phase. Concentrations were estimated using standard curves.

3. Results and discussion

3.1. Activities of inducible and constitutive promoters in Pseudomonas putida

To facilitate promoter selection, two inducible and four constitutive promoters were first evaluated. The inducible ParaB and PrhaB promoters were selected for their low basal expression and high inducible expression in *P. putida* KT2440 [30]. Four constitutive promoters with diverse promoter strength in *C. necator* H16 [28] were also studied.

Results showed cell growth to be unaffected by the introduction of plasmids in this promoter test (Figure S3). Activities of the promoters were compared based on the expression of green fluorescent protein (GFP; for inducible promoters) and red fluorescent protein (RFP; for constitutive promoters) achieved in *P. putida* (Fig. 1). Both inducible promoters exhibited minimal basal expression throughout the 72-h cultivation period (Fig. 1a). When induced, ParaB displayed higher promoter activities compared to PrhaB, confirmed by a two-way ANOVA analysis (α =0.05, P < 0.01). Interestingly, the fluorescence decreased after maximum fluorescence was detected at 8 h (ParaB) and 12 h (PrhaB), suggesting the loss of promoter activity. A previous study by Carelo et al. demonstrated that both ParaB and PrhaB promoters rapidly reached maximal expression of the fluorescent protein following induction, consistent with the observations reported in this study [30]. Loss of promoter activity over time can be attributed to numerous factors, including plasmid instability and loss during prolong cultivation [31], transcriptional regulation of the virulence factor regulator [32], insufficient inducer uptake due to the absence of specific rhamnose transporters [33] or a combination of these factors.

In contrast to the inducible promoters, the constitutive promoters showed stable activities throughout the cultivation period (Fig. 1b). Promoter Pg25 had the highest activity followed by Pj5, while the activities of PrrsC and PphaC1 were very low. Compared to inducible promoters, the constitutive promoters exhibited greater variability between replicates. This is likely due to their inherent sensitivity of protein expression to the cellular growth state and a lack of external regulatory mechanism. Their relative promoter activities are similar to that previously observed in $C.\ necator$, where they have decreasing activities in the order of Pg25 > Pj5 > PrrsC > PphaC1 in $C.\ necator\ H16$ [28]. This is also the first demonstration of these constitutive promoters in $P.\ putida$, adding new promoter elements to the molecular toolkit for this microbe.

Promoters ParaB and PrhaB offer the advantage of precise control over the timing and level of expression with minimal basal expression, enabling activation on demand. In contrast, constitutive promoters provide consistent expression levels across a range of cultivation conditions. To investigate the impact of both types of promoters, ParaB, PrhaB and PphaC1 were selected for subsequent work.

3.2. PHA blend composition was modulated by promoter selection

The pathway for P(3HB) production was introduced into *P. putida* by the addition of three enzymes, PhaA, PhaB and PhaC, via the *phaCAB* operon from the bacterium *Cupriavidus necator* H16 (Figure S1). Plasmids with promoters ParaB, PrhaB and PphaC1 driving heterologous expression of the *phaCAB* operon led to the production of P(3HB) and mcl-PHA blends (Fig. 2), as confirmed by gas chromatography analysis. The native *P. putida* produced mcl-PHA with 3-hydroxydecanoate as the major monomer (Fig. 2a), consistent with previous reports [34,35]. Addition of the heterologous *phaCAB* operon resulted in PHA blends

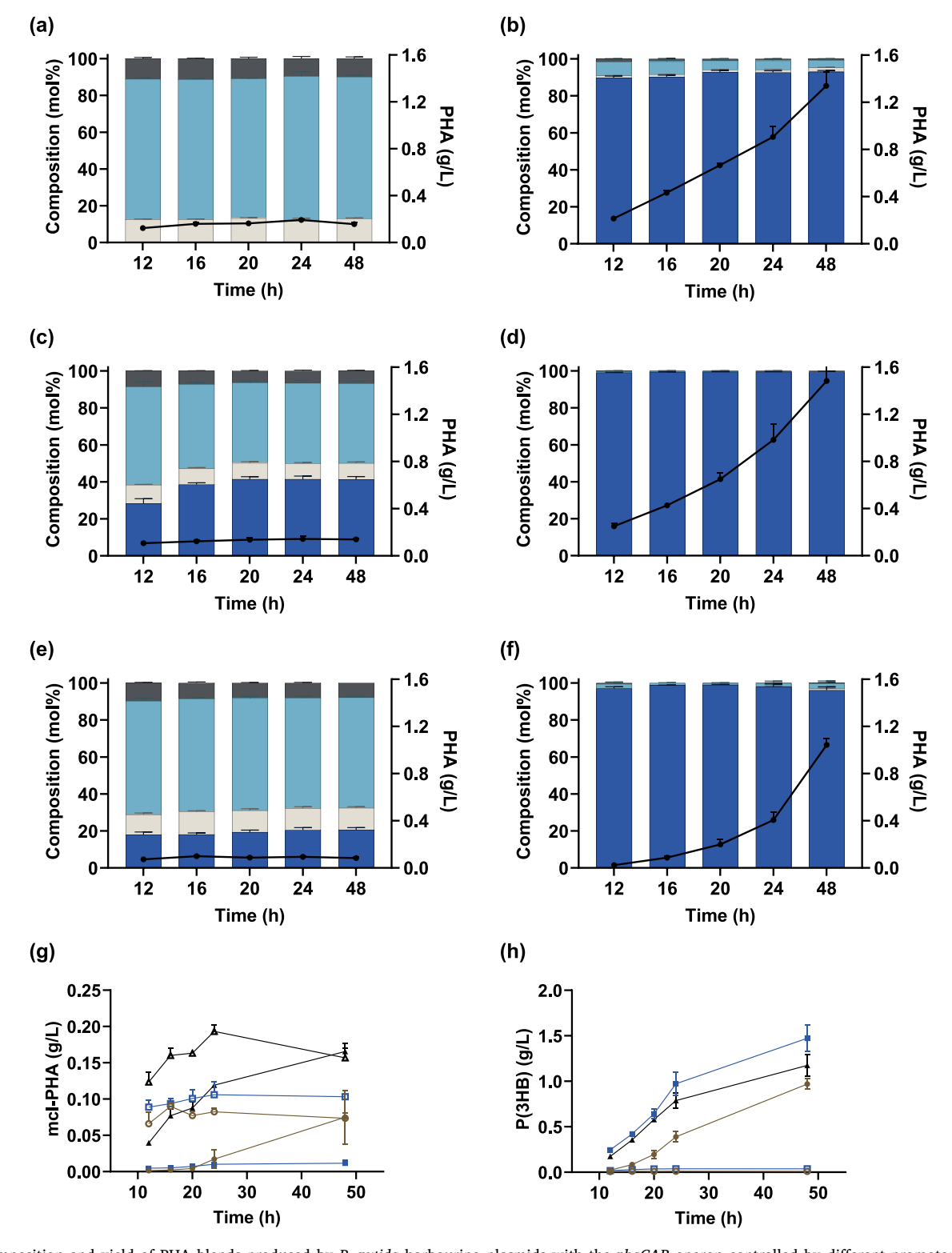
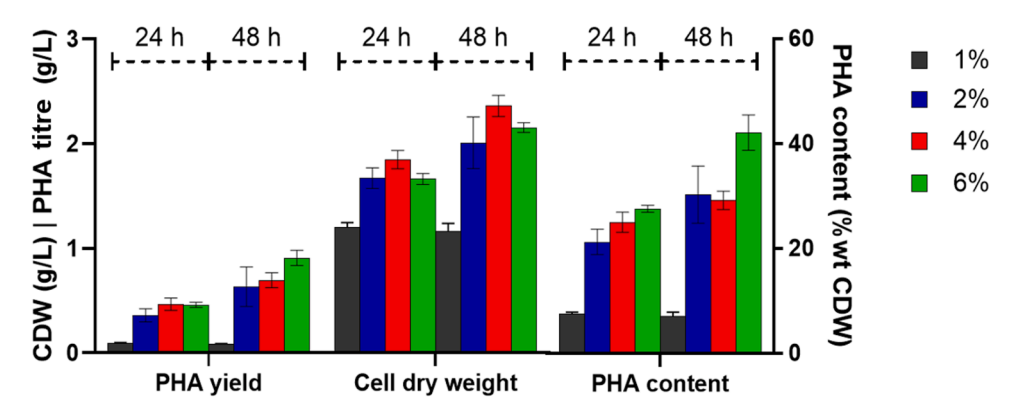


Fig. 2. Composition and yield of PHA blends produced by *P. putida* harbouring plasmids with the *phaCAB* operon controlled by different promoters. PHA was produced in MSM with 1 %(w/v) glucose. (a-f) Black line indicates the PHA titre. The bar chart shows the monomer composite for C4: ____, C6: ____, C6: ____, C10: ____, C12: ____. (a) No plasmid; (b) PphaC1; (c) ParaB (basal); (d) ParaB (induced); (e) PrhaB (basal); (f) PrhaB (induced). Component yields of (g) mcl-PHA and (h) P (3HB); no plasmid (black, open triangle), PphaC1 (black, closed triangle), ParaB [blue, open (basal) and closed (induced) square], PrhaB [brown, open (basal) and closed (induced) circles].

with 17.9 mol% to 99.6 mol% of 3HB monomer, depending on the promoter used (Fig. 2b-f).

Surprisingly, non-induced ParaB and PrhaB promoters produced PHA blends with 17.9 – 41.5 mol% of 3HB monomer (Figs. 2c and 2e),

despite their low basal activities. Promoter PphaC1 with low activity also produced PHA with 89.7-93.0 mol% of 3HB monomer (Fig. 2b). These high P(3HB) compositions appear inconsistent with the promoters' minimal activities characterised in Fig. 1. However it is



 $\textbf{Fig. 3.} \ \ PHA \ produced \ by \ \textit{P. putida} \ \ with \ the \ \textit{phaCAB} \ operon \ controlled \ by \ basal \ activity \ of \ PrhaB. \ Cells \ were \ cultivated \ in \ MSM \ with \ 1\%-6\%(w/v) \ of \ glucose.$

Table 2
PHA production by *P. putida* using various feedstock. The PHA content and yield for this study were from cells cultivated in MSM with 1 %(w/v) glucose for 48 h.

Blend (composition, mol%)	Strain (Plasmid)	Feedstock	PHA content (wt% CDW)	Yield (g PHA / g feedstock)	Reference
Flask culture					
mcl-PHA (100)	P. putida KT2442	Sodium octanoate	66.21	0.187	[45]
mcl-PHA (100)	P. putida KT2440 Δupp	Glucose	22.1	0.03	[44]
mcl-PHA (100)	P. putida KT2440	Glucose	32.1	0.08	[42]
mcl-PHA(100)	P. putida mt-2	Glucose	12.3 ± 0.88	0.015 ± 0.002	This study
PHB:mcl-PHA	P. putida mt-2	Glucose	$\textbf{48.2} \pm \textbf{2.2}$	0.134 ± 0.012	This study
(93.0:7.0)	(PphaC1k-phaCAB)				
PHB:mcl-PHA	P. putida mt-2	Glucose	11.7 ± 0.5	$\textbf{0.014} \pm \textbf{0.001}$	This study
(41.2:58.8)	(basal ParaB-phaCAB)				
PHB:mcl-PHA	P. putida mt-2	Glucose	$\textbf{52.2} \pm \textbf{4.3}$	0.148 ± 0.015	This study
(99.6:0.4)	(induced ParaB-phaCAB)				
PHB:mcl-PHA	P. putida mt-2	Glucose	$\textbf{7.2} \pm \textbf{0.7}$	0.008 ± 0.001	This study
(20.6:79.4)	(basal PrhaB-phaCAB)				
PHB:mcl-PHA	P. putida mt-2	Glucose	$\textbf{45.3} \pm \textbf{2.7}$	0.105 ± 0.005	This study
(96.1:3.9)	(induced PrhaB-phaCAB)				
Fed-batch fermentation					
mcl-PHA (100)	P. putida KT2440	Crude glycerol	21.4	0.08	[34]
mcl-PHA (100)	P. putida ΔphaZ	Crude glycerol	27.2	0.100	[34]
mcl-PHA (100)	P. putida KT2440	Acetate	22	0.02	[58]
mcl-PHA (100)	P. putida KT2440	Acetate	43	0.03	[58]
	(induced pBBR1-acs)				
mcl-PHA (100)	P. putida KT2440	Nonanoic acid	32	0.56	[46]
Batch fermentation					
PHB:mcl-PHA (64:36)	P. citronellolis NRRL B-2504 and C. necator H16	Sugar in apple pulp waste	33.6	0.109	[23]

Table 3PHA produced by native and engineered *P. putida* with different plasmids and extracted using the Soxhlet. The plasmids carry the *phaCAB* operon under the control of different promoters. *P. putida* cells were collected from 400 mL of culture after 24 h of cultivation.

Promoter	Monomer composition (mol%)			CDW (g/L)	PHA content (wt% CDW)	PHA Titre (g/L)		
	C4	C6	C8	C10	C12			
No plasmid	n.d.	1.6 ± 0.0	14.2 ± 0.5	74.1 ± 0.2	10.1 ± 0.3	1.45 ± 0.07	18.1 ± 2.9	0.263 ± 0.054
ParaB (basal)	81.4 ± 3.1	0.4 ± 0.1	3.4 ± 0.4	12.9 ± 2.2	1.9 ± 0.4	1.48 ± 0.06	16.0 ± 2.3	0.238 ± 0.043
PrhaB (basal)	30.4 ± 12.5	1.1 ± 0.3	9.6 ± 2.2	51.3 ± 9.0	7.5 ± 1.0	1.29 ± 0.06	10.5 ± 0.6	0.136 ± 0.013
ParaB (induced)	99.0 ± 0.3	n.d.	0.4 ± 0.0	0.7 ± 0.3	n.d.	1.88 ± 0.05	44.3 ± 2.7	0.829 ± 0.030
PrhaB (induced)	99.2 ± 0.2	n.d.	0.5 ± 0.1	0.5 ± 0.1	n.d.	1.86 ± 0.02	38.5 ± 5.3	0.716 ± 0.104
PphaC1	$\textbf{95.5} \pm \textbf{0.7}$	n.d.	$\textbf{1.0} \pm \textbf{0.1}$	$\textbf{3.0} \pm \textbf{0.5}$	$\textbf{0.6} \pm \textbf{0.1}$	$\textbf{2.44} \pm \textbf{0.03}$	42.3 ± 3.0	1.031 ± 0.061

n.d. = not detected.

important to note that protein expression is influenced by both transcriptional and translational processes. Same transcriptional levels for different targets (i.e. fluorescent protein and PhaCAB) can yield different protein expression levels depending on their respective mRNA structure, stability and the tRNA pool in the cell [36]. Protein degradation rates also vary between proteins, further influencing their intracellular concentrations [37,38]. Moreover, PHB production differs fundamentally from fluorescent protein expression (Fig. 1). For PhaCAB (Figs. 2b, 2c

and 2e), leaky expression may be sufficient to produce levels of biosynthetic enzymes, which can continuously catalyse substrate turnover and drive PHB synthesis. Thus the observed PHB accumulation is likely a cumulative, multi-turnover outcome, instead of just the effect of transcription and translation. Upon induction of ParaB and PrhaB, the PHA produced was composed almost entirely of 3HB monomers (Figs. 2d and 2f).

New BIOTECHNOLOGY 88 (2025) 161-170

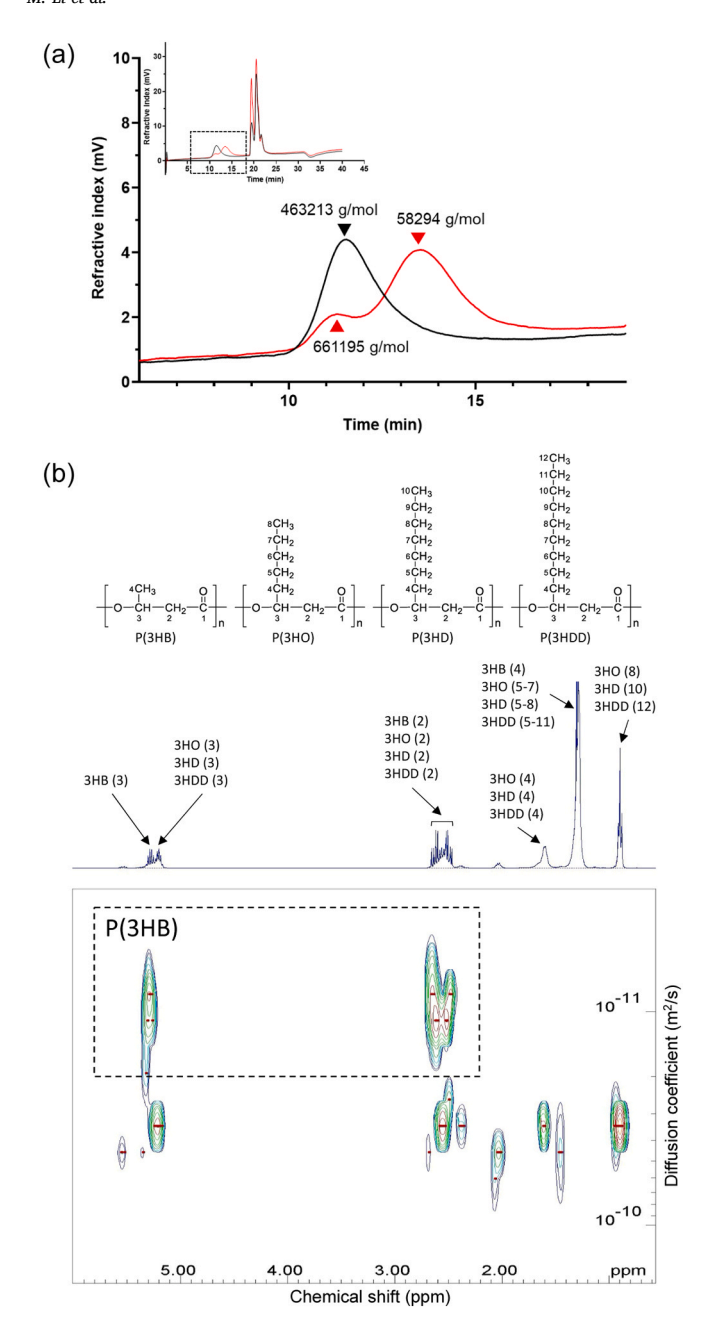


Fig. 4. Characteristics of Soxhlet extracted PHA blend produced by *P. putida* carrying the plasmid PrhaB-phaCAB. (a) Gel permeation chromatography of PHA produced under basal (red line) and induced (black line) conditions. The inset shows the complete chromatogram with the magnified region marked in a dotted rectangle. Molecular weights of peaks are indicated in the diagram. (b) DOSY NMR analysis of PHA blends from PrhaB (basal) with $30.4 \pm 12.5 \text{ mol}\%$ of 3HB. The diffusion coefficient of P(3HB) and mcl-PHA are distinct.

3.3. Promoter selection and carbon feedstock affected PHA titre

For native *P. putida* (Fig. 2a), the PHA titre peaked at 0.193 g/L of mcl-PHA after 24 h of cultivation. Compared to all engineered strains, this was the highest mcl-PHA titre achieved. Notably, its PHA content decreased as cultivation time increased from 24 h to 48 h (Fig. 2g), likely due to the mobilization of stored mcl-PHA by the native PHA depolymerase (PhaZ) in *P. putida* cells [39]. This *phaZ* gene is located within a gene cluster, situated between the *phaC1* and *phaC2* genes, and specifically hydrolyses mcl-PHAs [40].

Compared to native *P. putida*, all engineered strains had lower mcl-PHA titres except the strain harbouring the PphaC1 construct, which showed comparable mcl-PHA titre at 48 h (Fig. 2g). When non-induced ParaB and PrhaB were used, the overall PHA titre decreased due to lower mcl-PHA production. For induced ParaB, induced PrhaB and constitutive PphaC1, the overall PHA titre was up to 7.7-fold higher than that of native *P. putida*. This increase was attributed to the continuous accumulation of P(3HB) during cultivation, achieving a maximum PHA titre of 1.04 – 1.48 g/L at 48 h (Tables S3, S5 and S7). Between these three constructs, induced ParaB showed the most increase in P(3HB) production and largest reduction in mcl-PHA titre (Figs. 2g and 2h). This was likely due to the competition for the same metabolite, acetyl-CoA, in both the native mcl-PHA and engineered P(3HB) pathways (Figure S1).

Among the three promoters and five conditions tested (Figs. 2a-2h), engineered P. putida with non-induced ParaB and PrhaB produced the most balanced PHA blends with 41.5 mol% and 20.5 mol% of P(3HB) respectively. To investigate if PHA titre can be increased while maintaining the blend composition, glucose concentration in the cultivation medium was increased from 1 % (w/v) to 6 % (w/v). The engineered strain with basal activity of PrhaB was selected for this test due to its relatively stable composition across all time points (Fig. 2e). PHA titre increase was most pronounced when glucose was elevated from 1 % (w/ v) to 2 % (w/v), due to a combination of both higher cell mass and increased PHA content. Rising glucose concentration from 1 % (w/v) to 6 % (w/v) in a 48-h cultivation led to more than 10-fold increase in PHA titre to 0.91 \pm 0.07 g/L and a PHA content of 42.2 wt% CDW (Fig. 3). This elevated PHA production favoured the P(3HB) component, where the PHA blend produced at 6 % (w/v) glucose was composed of 90.4 \pm 0.9 mol% 3HB, compared to the 20.6 \pm 1.2 mol% when cultivated in medium with 1 %(w/v) glucose. This change in blend composition underscored the challenge and importance of simultaneous control of both pathways for mcl-PHA and P(3HB) synthesis. While P(3HB) synthesis is dependent only on the availability of acetyl-CoA (Figure S1) in this study, mcl-PHA is derived from β-oxidation and de novo fatty acid biosynthesis which are tightly regulated in the cell's central carbon metabolism [41].

A broad range of PHA yield from *P. putida* had been reported in literature (0.02–0.187 g PHA/ g feedstock; Table 2), depending on the feedstock, cultivation conditions and strain used. We achieved PHA blends yields of 0.148 g PHA/ g glucose, which is higher than the 0.109 g/ g feedstock previously obtained from co-cultivation of *P. citronellolis* NRRL B-2504 and *C. necator* H16 [23]. Native *P. putida* produced 0.015 g PHA/ g glucose in this study, consistent with 0.02–0.08 g PHA/ g feedstock reported for derivatives of *P. putida* KT2440 mt-2 [42–44]. Strategies such as fed-batch fermentation, optimized feeding regimes, and the addition of medium-chain-length PHA (mcl-PHA) precursors have been shown to enhance cell density and PHA yield in *P. putida* (Table 2) [45–47]. These methods could be integrated with our engineered *P. putida* strain to further improve PHA blend titre and yield.

3.4. The P(3HB) and mcl-PHA components had different molecular weights

To verify a PHA blend is produced instead of a co-polymer, the total PHA was Soxhlet extracted from cells and analysed using a combination of GPC and NMR. The purified PHA had titre and composition (Table 3) similar to results from GC analysis of lyophilised cells (Tables S2–S7), validating the robustness of our methods. Monomer 3-hydroxyhexanoate was detected in some samples at low levels of 0.4-1.6 mol%. This was not detected during analysis of the lyophilised cells, likely due to lower sensitivity of the method.

Gel permeation chromatography (GPC) analysis showed the molecular weight of mcl-PHA produced by native *P. putida* was 71.5 \pm 4.2 kg/mol (Table S8), within the broad weight-average molecular weights of 69 kg/mol to 111 kg/mol previously reported for *P. putida* [45,48,49]. For PphaC1, ParaB (induced), and PrhaB (induced) promoters where the produced PHA had at least 95.5 \pm 0.7 mol% of 3HB (Table 3), GPC

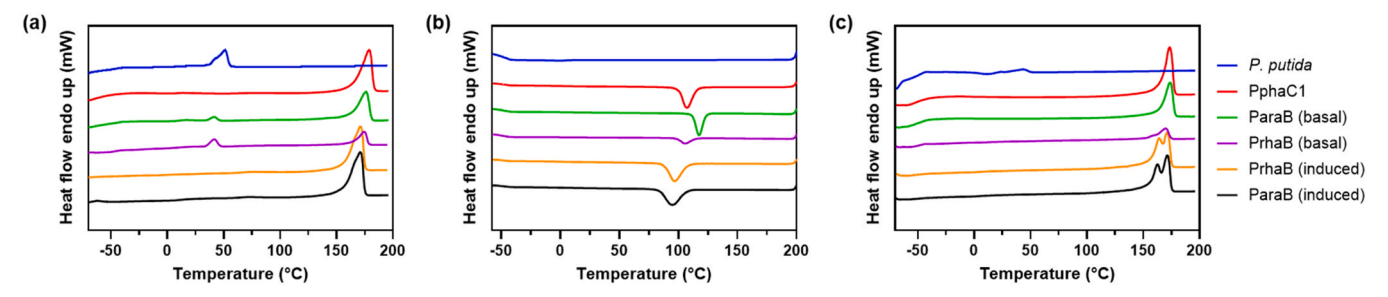


Fig. 5. DSC thermograms recorded during (a) first heating, (b) cooling and (c) second heating of purified mcl-PHA and PHA blends produced respectively by native and engineered *P. putida*.

Table 4Thermal properties of PHA blends produced via different methods.

Blend composition			Thermal properties (°C)			
(mol%)	Production method	Carbon source	T _c	T_c T_m T_d		Reference
PHB:PHO (79:21)*	Melt compounding	n.a.	78	177	n.r.	[17]
PHB:mcl-PHA (64:36)*	Co-culture of C. necator and P. citronellolis	apple pulp waste	n.r.	T _{m1} : 52 T _{m2} : 174	297	[23]
PHB:mcl-PHA (80:20)	P. putida + phaCAB on plasmid	0.5 % (w/v) octanoate 0.5 % (w/v) gluconate	n.r.	143	n.r.	[59]
PHB:mcl-PHA (35:65)	P. putida + phaCAB on plasmid	0.1 % (w/v) octanoate 0.9 % (w/v) gluconate	n.r.	153	n.r.	[59]
PHB:mcl-PHA (81.4:18.6)	P. putida + ParaB-phaCAB on plasmid (non-induced)	1.0 % (w/v) glucose	$117.6 \\ \pm 0.1$	$174.7 \\ \pm 0.8$	$\textbf{287.4} \pm \textbf{2.1}$	This study
PHB:mcl-PHA (30.4:69.6)	<i>P. putida</i> + PrhaB- <i>phaCAB</i> on plasmid (non-induced)	1.0 % (w/v) glucose	$\begin{array}{c} 107.3 \\ \pm \ 1.6 \end{array}$	$171.4 \\ \pm 1.6$	$\begin{array}{c} 290.4 \\ \pm \ 11.1 \end{array}$	This study

^{*} Calculated value; n.a. = not applicable; n.r. = not reported.

showed one main peak with molecular weights ranging from 298.3 \pm 44.9 kg/mol to 502.2 \pm 50.6 kg/mol. This is 4–7 times higher than the molecular weight of the mcl-PHA. Compared to induced ParaB and PrhaB, the P(3HB) from non-induced ParaB and PrhaB had molecular weights that were respectively 56.4 % and 71.8 % higher. This higher molecular weight of P(3HB) is likely attributed to the lower PhaC concentration in the cell [50].

The PHA blends produced with ParaB (basal) and PrhaB (basal) promoters exhibited two species with distinct molecular weights on GPC (Fig. 4a). Diffusion-ordered spectroscopy (DOSY) was employed to identify these species. DOSY differentiates NMR signals from different molecules by their different molecular translational diffusion rate. Two diffusion coefficients of 1.2×10^{-11} m²/s and 3.7×10^{-11} m²/s were derived for the PHA sample from non-induced PrhaB (Fig. 4b). These corresponded to P(3HB) as the larger molecule and mcl-PHA as the smaller molecule respectively (Table S8), confirming a PHA blend.

3.5. Thermal properties of the PHA blends

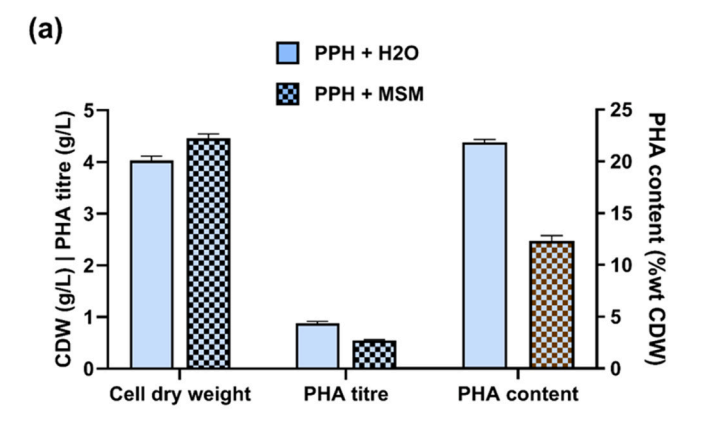
The thermal properties of the PHA blends produced in this work were measured for comparison to similar blends produced using other methods. The produced PHA blends showed a single thermal degradation event in TGA, with T_d between $287.0-298.3\,^{\circ}\text{C}$ (Table S9, Figure S4). A one-way ANOVA analysis showed no significant difference in the T_d of all PHA samples measured. Crystallization peaks from DSC results were observed between 98°C and 118°C on cooling from the first melt, except for the mcl-PHA from *P. putida* (Fig. 5b). Mcl-PHA is typically amorphous and does not develop crystalline phase during cooling [51,52], which explains the absence of a distinct crystallization peak. It also has a melting temperature of $43.7\pm0.1^{\circ}\text{C}$ (Fig. 5c, Table S9), which is characteristic of mcl-PHA from *Pseudomonas* species [53]. All other samples had T_m between 163°C to 175°C (Fig. 5c, Table S9), similar to scl-PHAs [53], with double melting peaks observed for

samples ParaB (induced) and PrhaB (induced). These double melting peaks were absent during the first heating (Fig. 5a) and likely originated from the melt-recrystallization resulting in reorganization of the polyester crystals, a phenomenon also reported for poly(ethylene terephthalate) [54] and poly(butylene succinate) [55]. These thermal properties were comparable to properties of similar PHA produced using melt compounding and through fatty acid precursor feeding during fermentation (Table 4).

3.6. Engineered P. putida produced PHA blend from potato peel hydrolysate

The potato peel hydrolysate had $172.7 \pm 6.5 \, \mathrm{mM}$ glucose and no measurable quantities of xylose was detected. The *P. putida* harbouring plasmid PrhaB-phaCAB grew in the potato peel hydrolysate media, even when the hydrolysate was diluted with water (1:1, v/v) without additional nutrients added (Fig. 6a). When the hydrolysate was supplemented with MSM medium (1:1, v/v), biomass accumulation increased marginally to achieve a maximum cell dry weight of 4.45 g/L (Fig. 6a). Despite an increased biomass, the cellular PHA content was 12.3 %wt CDW, about half of that produced when no MSM was added (Fig. 6a). This was likely due to the additional nitrogen supplied by MSM, which lowered the C/N ratio to create conditions less favourable for PHA accumulation. The PHA blend accumulated comprised predominantly P (3HB), with a minor fraction of mcl-PHA. The molar fraction of 3HB ranged from 85.8 to 95.7 mol% (Fig. 6b), similar to PHA blends when only MSM with glucose was used (Fig. 2f).

A key challenge in PHA production is the high cost of feedstock. Potato peels, with an anticipated global production of 8 million tonnes annually by 2030 [56], represent a promising low-cost, high-volume alternative. Previous studies have demonstrated PHA production from potato peels using *Bacillus circulans* [57], where 0.1 g/mL of dried peel powder yielded 10 g/L of reducing sugars via hydrochloric acid



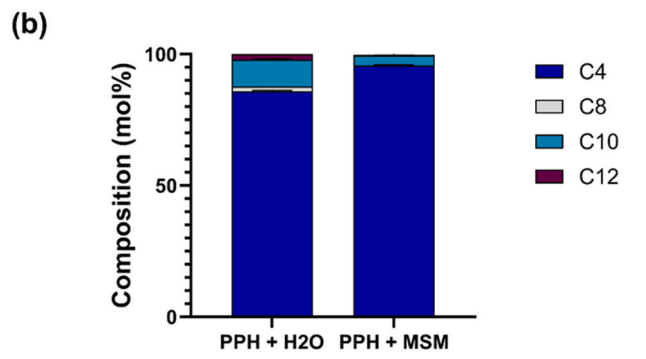


Fig. 6. Characterisation of PHA production by engineered *P. putida* cultivated in potato peel hydrolysate (PPH) based media. Data collected after 24 h of cultivation in either PPH and $\rm H_2O$ or PPH and MSM. (a) Comparison of PHA titre (g/L), cell dry weight (CDW, g/L), and PHA content (% CDW) and (b) PHA monomer composition determined by GC analysis of lyophilised cells. The strain used in both medium was *P. putida* expressing the *phaCAB* operon under basal activity of the PrhaB promoter.

hydrolysis at 121 $^{\circ}$ C. In contrast, our enzymatic hydrolysis approach produced 31.1 g/L of glucose. The variation in sugar yield is likely influenced by differences in peel origin and moisture content, in addition to the hydrolysis method. Overall, our findings confirm that the engineered *P. putida* can utilise potato peel hydrolysate as a low-cost feedstock for PHA production.

4. Conclusion

This study showed direct microbial synthesis of PHA blend using $P.\ putida$ and is a first demonstration of blend composition control using different promoters. We generated P(3HB) and mcl-PHA blends with 3HB content ranging from 17.9 mol% to 99.6 mol%. The highest PHA titre of 1.48 ± 0.15 g/L and a PHA content of 52.2 ± 4.3 wt% CDW was obtained when the phaCAB operon was controlled by the induced ParaB promoter in a 48-h cultivation. The work also identified four new constitutive promoters for $P.\ putida$, adding to the molecular toolkit for this microbe.

Key factors identified to influence blend composition during direct microbial synthesis include; (1) The tightly regulated native mcl-PHA pathwaysand PhaZ depolymerase in *P. putida* restricted the production of mcl-PHA. (2) Promoters can regulate the introduced pathway for P (3HB) synthesis to vary the PHA blend composition. (3) Increasing glucose concentration in the medium increased PHA titre by more than 10-fold and favoured P(3HB) synthesis in the blend. (4) PHA blends produced in this work have thermal properties comparable to similar blends produced by melt compounding, co-culture of two microorganisms and precursor feeding during fermentation. The outcome from this study validated microbial blend synthesis and control via promoter

selection, paving the way to a simple one-step biomanufacturing of customizable PHA blends. These findings further established a feasible framework for engineering other PHA-producing microorganisms, including gram-negative bacteria to enable the production of lipopoly-saccharide free PHA for clinical applications.

Declaration of Competing Interest

The authors declare that they have no known competing financial interests or personal relationships that could have appeared to influence the work reported in this paper.

Acknowledgements

This work was supported by the EPSRC New Investigator Award (EP/X025853/1). We thank the Standard European Vector Architecture (SEVA) and Prof. Alex Nielson (Technical University of Denmark) for sharing the plasmids pPS85 and pPS87. We also thank Mr. Alan Burling from The University of Sheffield (School of Mathematical and Physical Sciences) for support in gel permeation chromatography.

Appendix A. Supporting information

Supplementary data associated with this article can be found in the online version at doi:10.1016/j.nbt.2025.05.004.

References

- Zytner P, et al. A review on polyhydroxyalkanoate (PHA) production through the use of lignocellulosic biomass. Rsc Sustain 2023;1:2120–34. https://doi.org/ 10.1039/d3su00126a.
- [2] Getino L, Martin JL, Chamizo-Ampudia A. A review of polyhydroxyalkanoates: characterization, production, and application from waste. Microorganisms 2024; 12. https://doi.org/10.3390/microorganisms12102028.
- [3] Kusuma HS, et al. Waste to wealth: Polyhydroxyalkanoates (PHA) production from food waste for a sustainable packaging paradigm. Food Chem (Oxf 2024;9:100225. https://doi.org/10.1016/j.fochms.2024.100225.
- [4] Zhou W, Bergsma S, Colpa DI, Euverink GW, Krooneman J. Polyhydroxyalkanoates (PHAs) synthesis and degradation by microbes and applications towards a circular economy. J Environ Manag 2023;341:118033. https://doi.org/10.1016/j. jenvman.2023.118033.
- [5] Palmeiro-Sanchez T, O'Flaherty V, Lens PNL. Polyhydroxyalkanoate bioproduction and its rise as biomaterial of the future. J Biotechnol 2022;348:10–25. https://doi.org/10.1016/j.jbiotec.2022.03.001.
- [6] Mai J, et al. Synthesis and physical properties of polyhydroxyalkanoate (PHA)based block copolymers: A review. Int J Biol Macromol 2024;263:130204. https://doi.org/10.1016/j.ijbiomac.2024.130204.
- [7] Buntinx M, Vanheusden C, Hermans D. Processing and properties of polyhydroxyalkanoate/ZnO nanocomposites: A review of their potential as sustainable packaging materials. Polym (Basel) 2024;16. https://doi.org/10.3390/ polym16213061.
- [8] Chen GQ, Jiang XR. Engineering microorganisms for improving polyhydroxyalkanoate biosynthesis. Curr Opin Biotechnol 2018;53:20–5. https://doi.org/10.1016/j.copbio.2017.10.008.
- [9] Foong CP, et al. A novel and wide substrate specific polyhydroxyalkanoate (PHA) synthase from unculturable bacteria found in mangrove soil. J Polym Res 2017;25. https://doi.org/10.1007/s10965-017-1403-4.
- [10] Fukui T, Doi Y. Cloning and analysis of the poly(3-hydroxybutyrate-co-3-hydroxyhexanoate) biosynthesis genes of *Aeromonas caviae*. J Bacteriol 1997;179: 4821–30. https://doi.org/10.1128/jb.179.15.4821-4830.1997.
- [11] Dufresne A, Vincendon M. Poly(3-hydroxybutyrate) and poly(3-hydroxyoctanoate) blends: Morphology and mechanical behavior. Macromolecules 2000;33: 2998–3008, https://doi.org/10.1021/ma991854a.
- [12] Matsumoto K, et al. Dynamic changes of intracellular monomer levels regulate block sequence of polyhydroxyalkanoates in engineered *Escherichia coli*. Biomacromolecules 2018;19:662–71. https://doi.org/10.1021/acs. biomac.7b01768.
- [13] Pederson EN, McChalicher CW, Srienc F. Bacterial synthesis of PHA block copolymers. Biomacromolecules 2006;7:1904–11. https://doi.org/10.1021/ bm0510101
- [14] Tappel RC, et al. Engineering Escherichia coli for improved production of short-chain-length-co-medium-chain-length poly[(R)-3-hydroxyalkanoate] (scl-mcl PHA) copolymers from renewable non-fatty acid feedstocks. ACS Sustain Chem Eng 2014:2:1879–87. https://doi.org/10.1021/sc500217p.
- [15] Phan HT, et al. Directed evolution of sequence-regulating polyhydroxyalkanoate synthase to synthesize a medium-chain-length-short-chain-length (MCL-SCL) block

- copolymer. Biomacromolecules 2022;23:1221–31. https://doi.org/10.1021/acs.biomac.lc01480
- [16] Basnett P, et al. Novel poly(3-hydroxyoctanoate)/poly(3-hydroxybutyrate) blends for medical applications. React Funct Polym 2013;73:1340–8. https://doi.org/ 10.1016/j.reactfunctpolym.2013.03.019.
- [17] Nerkar M, Ramsay JA, Ramsay BA, Kontopoulou M. Melt compounded blends of short and medium chain-length poly-3-hydroxyalkanoates. J Polym Environ 2014; 22:236–43. https://doi.org/10.1007/s10924-013-0635-6.
- [18] Deng Y, et al. Poly(hydroxybutyrate-co-hydroxyhexanoate) promoted production of extracellular matrix of articular cartilage chondrocytes *in vitro*. Biomaterials 2003;24:4273–81. https://doi.org/10.1016/s0142-9612(03)00367-3.
- [19] Deng Y, Zhao K, Zhang XF, Hu P, Chen GQ. Study on the three-dimensional proliferation of rabbit articular cartilage-derived chondrocytes on polyhydroxyalkanoate scaffolds. Biomaterials 2002;23:4049–56. https://doi.org/ 10.1016/s0142-9612(02)00136-9.
- [20] Zhao K, Deng Y, Chun Chen J, Chen GQ. Polyhydroxyalkanoate (PHA) scaffolds with good mechanical properties and biocompatibility. Biomaterials 2003;24: 1041–5. https://doi.org/10.1016/s0142-9612(02)00426-x.
- [21] Ryu HW, Hahn SK, Chang YK, Chang HN. Production of poly(3-hydroxybutyrate) by high cell density fed-batch culture of *Alcaligenes eutrophus* with phosphate limitation. Biotechnol Bioeng 1997;55:28–32. https://doi.org/10.1002/(SICI) 1097-0290(19970705)55:1
- [22] Cerrone F, et al. Pseudomonas umsongensis GO16 as a platform for the in vivo synthesis of short and medium chain length polyhydroxyalkanoate blends. Bioresour Technol 2023;387:129668. https://doi.org/10.1016/j. biortech.2023.129668.
- [23] Rebocho AT, et al. Preparation and characterization of films based on a natural P (3HB)/mcl-PHA blend obtained through the co-culture of Cupriavidus necator and Pseudomonas citronellolis in apple pulp waste. Bioeng (Basel) 2020;7:34. https://doi.org/10.3390/bioengineering7020034.
- [24] Chen Z, et al. Synthesis of short-chain-length and medium-chain-length polyhydroxyalkanoate blends from activated sludge by manipulating octanoic acid and nonanoic acid as carbon sources. J Agric Food Chem 2018;66:11043–54. https://doi.org/10.1021/acs.jafc.8b04001.
- [25] Ankenbauer A, et al. KT2440 is naturally endowed to withstand industrial-scale stress conditions. Microb Biotechnol 2020;13:1145–61. https://doi.org/10.1111/ 1751-7015 13571
- [26] Schlegel HG, Kaltwasser H, Gottschalk G. Ein submersverfahren zur kultur wasserstoffoxydierender bakterien - wachstumsphysiologische untersuchungen. Arch Fur Mikrobiol 1961;38:209–22. https://doi.org/10.1007/Bf00422356.
- [27] Cho JH, Kim EK, So JS. Improved transformation of *Pseudomonas putida* KT2440 by electroporation. Biotechnol Tech 1995;9:41–4. https://doi.org/10.1007/ Bf00152998
- [28] Johnson AO, Gonzalez-Villanueva M, Tee KL, Wong TS. An engineered constitutive promoter set with broad activity range for *Cupriavidus necator* H16. ACS Sythn Biol 2018;7:1918–28. https://doi.org/10.1021/acssynbio.8b00136.
- [29] Kovach ME, et al. Four new derivatives of the broad-host-range cloning vector pBBR1MCS, carrying different antibiotic-resistance cassettes. Gene 1995;166: 175-6. https://doi.org/10.1016/0378-1119(95)00584-1.
- [30] Calero P, Jensen SI, Nielsen AT. Broad-host-range ProUSER vectors enable fast characterization of inducible promoters and optimization of p-coumaric acid production in Pseudomonas putida KT2440. ACS Sythn Biol 2016;5:741–53. https:// doi.org/10.1021/acssynbio.6b00081.
- [31] Wegerer A, Sun T, Altenbuchner J. Optimization of an E. coli L-rhamnose-inducible expression vector: test of various genetic module combinations. BMC Biotechnol 2008;8:2. https://doi.org/10.1186/1472-6750-8-2.
- [32] McMackin EAW, et al. Cautionary notes on the use of arabinose- and rhamnoseinducible expression vectors in *Pseudomonas aeruginosa*. J Bacteriol 2021;203: e0022421. https://doi.org/10.1128/JB.00224-21.
- [33] Jeske M, Altenbuchner J. The Escherichia coli rhamnose promoter rhaP(BAD) is in Pseudomonas putida KT2440 independent of Crp-cAMP activation. Appl Microbiol Biotechnol 2010;85:1923–33. https://doi.org/10.1007/s00253-009-2245-8.
- [34] Borrero-de Acuna JM, et al. Production of medium chain length polyhydroxyalkanoate in metabolic flux optimized *Pseudomonas putida*. Microb Cell Fact 2014;13:88. https://doi.org/10.1186/1475-2859-13-88.
- [35] Sharma PK, Fu J, Cicek N, Sparling R, Levin DB. Kinetics of medium-chain-length polyhydroxyalkanoate production by a novel isolate of *Pseudomonas putida* LS46. Can J Microbiol 2012;58:982–9. https://doi.org/10.1139/w2012-074.
- [36] Gingold H, Pilpel Y. Determinants of translation efficiency and accuracy. Mol Syst Biol 2011;7:481. https://doi.org/10.1038/msb.2011.14.
- [37] Nordholt N, van Heerden J, Kort R, Bruggeman FJ. Effects of growth rate and promoter activity on single-cell protein expression. Sci Rep 2017;7:6299. https://doi.org/10.1038/s41598-017-05871-3.
- [38] Schikora-Tamarit MA, et al. Promoter activity buffering reduces the fitness cost of misregulation. Cell Rep 2018;24:755–65. https://doi.org/10.1016/j. celrep.2018.06.059.

- [39] Manoli MT, Nogales J, Prieto A. Synthetic control of metabolic states in Pseudomonas putida by tuning polyhydroxyalkanoate cycle. Mbio 2022;13:e01794-01721. https://doi.org/10.1128/mbio.01794-21.
- [40] de Eugenio LI, et al. Biochemical evidence that phaZ gene encodes a specific intracellular medium chain length polyhydroxyalkanoate depolymerase in Pseudomonas putida KT2442: Characterization of a paradigmatic enzyme. J Biol Chem 2007;282:4951–62. https://doi.org/10.1074/jbc.M608119200.
- [41] Mezzina MP, Manoli MT, Prieto MA, Nikel PI. Engineering native and synthetic pathways in *Pseudomonas putida* for the production of tailored polyhydroxyalkanoates. Biotechnol J 2021;16:e2000165. https://doi.org/ 10.1002/biot.202000165.
- [42] Davis R, et al. Conversion of grass biomass into fermentable sugars and its utilization for medium chain length polyhydroxyalkanoate (mcl-PHA) production by *Pseudomonas* strains. Bioresour Technol 2013;150:202–9. https://doi.org/ 10.1016/j.biortech.2013.10.001.
- [43] de Lorenzo V, Perez-Pantoja D, Nikel PI. Pseudomonas putida KT2440: the long journey of a soil-dweller to become a synthetic biology chassis. J Bacteriol 2024; 206:e0013624. https://doi.org/10.1128/jb.00136-24.
- [44] Zhang Y, et al. A promoter engineering-based strategy enhances polyhydroxyalkanoate production in *Pseudomonas putida* KT2440. Int J Biol Macromol 2021;191:608–17. https://doi.org/10.1016/j.ijbiomac.2021.09.142
- [45] Cai L, Yuan MQ, Liu F, Jian J, Chen GQ. Enhanced production of medium-chain-length polyhydroxyalkanoates (PHA) by PHA depolymerase knockout mutant of *Pseudomonas putida* KT2442. Bioresour Technol 2009;100:2265–70. https://doi.org/10.1016/j.biortech.2008.11.020.
- [46] Davis R, et al. High cell density cultivation of *Pseudomonas putida* KT2440 using glucose without the need for oxygen enriched air supply. Biotechnol Bioeng 2015; 112:725–33. https://doi.org/10.1002/bit.25474.
- [47] Poblete-Castro I, Rodriguez AL, Lam CM, Kessler W. Improved production of medium-chain-length polyhydroxyalkanoates in glucose-based fed-batch cultivations of metabolically engineered *Pseudomonas putida* strains. J Microbiol Biotechnol 2014;24:59–69. https://doi.org/10.4014/jmb.1308.08052.
- [48] de Vrije T, Nagtegaal RM, Veloo RM, Kappen FHJ, de Wolf FA. Medium chain length polyhydroxyalkanoate produced from ethanol by *Pseudomonas putida* grown in liquid obtained from acidogenic digestion of organic municipal solid waste. Bioresour Technol 2023;375:128825. https://doi.org/10.1016/j. biortech.2023.128825.
- [49] Nur-A-Tomal MS, et al. Tailoring feedstocks for enhanced medium-chain-length polyhydroxyalkanoate production and biomedical nanoemulsion applications. ACS Sustain Chem Eng 2024;12:14590–600. https://doi.org/10.1021/ acssuschemeng.4c02156.
- [50] Tsuge T. Fundamental factors determining the molecular weight of polyhydroxyalkanoate during biosynthesis. Polym J 2016;48:1051–7. https://doi. org/10.1038/pj.2016.78.
- [51] Kim DY, Kim HW, Chung MG, Rhee YH. Biosynthesis, modification, and biodegradation of bacterial medium-chain-length polyhydroxyalkanoates. J Microbiol 2007;45:87–97.
- [52] Nigmatullin R, et al. Medium chain length polyhydroxyalkanoates as potential matrix materials for peripheral nerve regeneration. Regen Biomater 2023;10: rbad063. https://doi.org/10.1093/rb/rbad063.
- [53] Mozejko-Ciesielska J, Szacherska K, Marciniak P. *Pseudomonas Species* as Producers of Eco-friendly Polyhydroxyalkanoates. J Polym Environ 2019;27:1151–66. https://doi.org/10.1007/s10924-019-01422-1.
 [54] Minakov AA, Mordvintsev DA, Schick C. Melting and reorganization of poly
- [54] Minakov AA, Mordvintsev DA, Schick C. Melting and reorganization of poly (ethylene terephthalate) on fast heating (1000 K/s). Polymer 2004;45:3755–63. https://doi.org/10.1016/j.polymer.2004.03.072.
- [55] Yasuniwa M, Tsubakihara S, Satou T, Iura K. Multiple melting behavior of poly (butylene succinate). II. Thermal analysis of isothermal crystallization and melting process. J Polym Sci, Part B: Polym Phys 2005;43:2039–47. https://doi.org/ 10.1002/polb.20499.
- [56] Ozer Uyar GE, Uyar B. Potato peel waste fermentation by *Rhizopus oryzae* to produce lactic acid and ethanol. Food Sci Nutr 2023;11:5908–17. https://doi.org/ 10.1002/fsn3.3670
- [57] Kag S, Kumar P, Kataria R. Potato Peel Waste as an Economic Feedstock for PHA Production by *Bacillus circulans*. Appl Biochem Biotechnol 2024;196:2451–65. https://doi.org/10.1007/s12010-023-04741-1.
- [58] Yang S, Li S, Jia X. Production of medium chain length polyhydroxyalkanoate from acetate by engineered *Pseudomonas putida* KT2440. J Ind Microbiol Biotechnol 2019;46:793–800. https://doi.org/10.1007/s10295-019-02159-5.
- [59] Shin HD, Lee JN, Lee YH. In vivo blending of medium chain length polyhydroxyalkanoates and polyhydroxybutyrate using recombinant Pseudomonas putida harboring phbCAB operon of Ralstonia eutropha. Biotechnol Lett 2002;24:1729–35. https://doi.org/10.1023/A:1020604915657.